

Crystallization kinetics of Ag-doped Se–Bi–Te chalcogenide glasses

Anup Kumar · P. B. Barman · Raman Sharma

Received: 12 July 2012 / Accepted: 12 February 2013 / Published online: 27 March 2013
© Akadémiai Kiadó, Budapest, Hungary 2013

Abstract Effect of Ag doping on the crystallization kinetics of amorphous $\text{Se}_{80.5}\text{Bi}_{1.5}\text{Te}_{18-y}\text{Ag}_y$ (for $y = 0, 1.0, 1.5,$ and 2.0 at.%) glassy alloys has been studied by differential scanning calorimetry (DSC). The DSC curves recorded at four different heating rates are analyzed to determine the transition temperature, activation energy, thermal stability, glass forming ability, and dimensionality of growth during phase transformation. Present study shows that the thermal stability and the glass-forming ability increase with an increase in the Ag content which is in agreement with the earlier studies. Our results show that $\text{Se}_{80.5}\text{Bi}_{1.5}\text{Te}_{16}\text{Ag}_2$ composition is thermally more stable and has a little tendency to crystallize in comparison to other compositions under study. The increase in thermal stability with increasing Ag concentration is attributed to an increase in the cohesive energy.

Keywords Chalcogenide glasses · Glass transition · Thermal stability · Glass forming ability · Non-isothermal · Avrami exponent

Introduction

Multinary amorphous semiconducting materials are of ample interest due to their abundant structural features and distinct properties. These materials contain characteristic features of disordered materials and some properties of crystalline semiconducting materials. Especially, the metallic chalcogenide glasses have received adequate attention due to their potential applications in active and passive thermoelectric, electronic, and optical devices [1]. They are emerging as promising materials with their use in optical memories and switching devices, electrophotography, X-ray and thermal imaging, ultra-high density phase change storage, biosensors, and are recently used as a core material in high efficiency fiber amplifiers [2–5]. The memory and threshold behavior of these materials is determined by their crystalline ability. Threshold switches are made near the center of glass-forming region and memory switches come from the boundaries of the glass-forming region. The materials which are stable and show little or no tendency to crystallize, when heated or cooled slowly, are vital in threshold switching while the materials that are more prone to crystallization have application in memory switching [6]. The glass structure and its thermal stability play an important role in their applications. Hence, the structural studies of chalcogenide materials are essential to understand the transport mechanisms and thermal stability [7]. Thermal stability of an amorphous chalcogenide alloys mean resistance to crystallization and is known in term of peak crystallization temperature (T_p). Technological applications of metallic glasses insist the stability of these materials with time and temperature. Consequently, it is significant to study the thermal stability, glass-forming ability (GFA), and to establish a suitable range of operating temperature for a specific technological application.

A. Kumar · R. Sharma (✉)
Department of Physics, Himachal Pradesh University,
Shimla 171005, India
e-mail: sramanb70@mailcity.com

A. Kumar
Department of Physics, Government Degree College,
Kullu, Himachal Pradesh, India

P. B. Barman
Department of Physics, Jaypee University of Information
Technology, Wahnaghat, Solan, Himachal Pradesh, India

The crystallization kinetics is an important tool to understand the atomic processes involved in the formation of crystalline phases. The most popular techniques used for studying the crystallization kinetics of non-isothermal transformation are differential scanning calorimetry (DSC) and differential thermal analysis (DTA). Out of these two techniques, DSC is preferred over DTA because it is simple, sensitive, easy to carry out [8], quick, and needs very small quantity of sample to measure the kinetic parameters [9]. The differential scanning calorimetric measurements in chalcogenide materials can be performed by any of these two methods: (i) isothermal and (ii) non-isothermal method [10]. In isothermal method, the material is quickly brought to a temperature above the glass transition temperature and the heat evolved is recorded as a function of time. On the other hand, in non-isothermal method, thermo-analytical method sample is heated at a constant rate and the heat evolved is recorded as a function of time or temperature. The non-isothermal method is preferred over the isothermal method due to its several advantages. Non-isothermal analysis experiments can be performed quickly and have wide temperature range as compared to the isothermal analysis. Non-isothermal crystallization kinetics can be performed by several methods [11–13] available in literature. In isothermal method, because of inherent transitions associated with the experimental setup, many of the phase transformations occur so rapidly to be measured. Therefore, the non-isothermal DSC technique has been widely used by the researchers to study the crystallization kinetics of chalcogenide glassy materials [14–20].

Among chalcogenide glasses, selenium (Se)-based glasses are preferred because of their unique properties in electronics, optics, and magnetism. From technological point of view pure *Se* has some shortcomings which can be overcome by alloying some elements to Se matrix. Addition of tellurium (Te) to selenium is known to improve the corrosion resistance property of selenium and reduce the electronic band gap of Se which makes the alloy important for technological applications. Due to their unique properties the Se–Te semiconducting alloys are of significant interest in various fields like sensors, laser materials, solar cells, infrared detectors, thermoelectric cooling materials [21], etc. But, the thermal instability leading to crystallization is one of the major drawbacks of these alloys. The addition of impurities, like Bi, Sn, Sb, Ag, etc., to these alloys is found to improve various properties like higher glass transition temperature, higher crystallization temperature, and thermal stability [22–24]. Addition of third element to the binary alloy helps in forming the cross linked structures thus increases the glass transition and crystallization temperature of the binary alloy. The insertion of Bi to Se–Te alloy has been seen to produce remarkable changes, like *p*- to *n*-type conduction [25, 26],

increase in chemical durability and broadening of the IR transparency region. But, at the same time it reduces the thermal stability of the material. On the other hand, silver (Ag) easily alloys by bridging the chalcogenide chains and makes the system stable [27]. Due to its ionic nature, addition of Ag results in various structural changes in the materials which in turn modify the band structure and hence electrical properties of the material. Due to their potential device applications in chemistry, optoelectronics, biology, and in optics such as in optical memories, micro lenses, waveguides, gratings, sensors, solid electrolytes, batteries, photo doping, etc. [28–32], Ag-containing chalcogenide glasses have received profuse attention in glass science and technology. They found applications in optical memory/holography material and membranes of sensors for potentiometric determination [10, 28, 33]. However, the present work seeks to study the effect of Ag on Se–Te-based quaternary glassy alloy. In Se-rich systems most of the researcher's have chosen the Se contents between 75 and 90 % which seems to be thermally stable thus a mid-way concentration of Se is chosen.

In the present work, an attempt has been made to study the crystallization kinetics of quaternary $\text{Se}_{80.5}\text{Bi}_{1.5}\text{Te}_{18-y}\text{Ag}_y$ chalcogenide glass by DSC technique under non-isothermal conditions. Non-isothermal DSC scans are performed at four different heating rates, i.e., at 2, 4, 8, and 12 K min^{-1} . Well-established theoretic models are used to analyze the data of investigated glassy alloys. The activation energy of glass transition has been evaluated by Kissinger's [34, 35] and Moynihan's method [36]. The crystallization process has been analyzed in terms of kinetic parameters, like Avrami exponent, dimensionality of growth, and activation energy of crystallization, using four different theoretic models proposed by Kissinger [34, 35], Augis and Bennett [37], Mahadevan et al. [38], and Matusita et al. [39]. Characteristic parameters, like thermal stability and GFA, are also computed from the heating rate dependence of glass transition temperature (T_g) and peak crystallization temperature (T_p).

Experimental

The glassy alloys of $\text{Se}_{80.5}\text{Bi}_{1.5}\text{Te}_{18-y}\text{Ag}_y$ (for $y = 0, 1.0, 1.5,$ and 2.0 at.%), in bulk form, were prepared by melt quenching technique. High purity (99.999 %) elemental substances were weighed according to their atomic percentages and were sealed in quartz ampoules (length ~ 6 cm and internal diameter ~ 8 mm) evacuated to a vacuum of 10^{-3} Pa, it avoids the reaction of the material with oxygen at higher temperature. The sealed ampoules were heated in a vertical furnace at an appropriate temperature of 1,323 K for 15 h by gradually increasing the temperature at the rate of

3–4 K min⁻¹. The ampoules were rocked frequently during heating to insure homogenization of the melt. After achieving the desired temperature and time the ampoules were rapidly quenched into ice cooled water. The samples of glassy material were separated from the ampoules by dissolving the ampoules in HF + H₂O₂ solution for about 48 h. The amorphous state of the bulk samples was confirmed by X-ray diffraction as no prominent peak was observed in the spectra. The crystallization behavior, in non-isothermal conditions, was investigated using a differential scanning calorimeter, Diamond Pyris (Perkin Elmer), with Al₂O₃ powder as reference material. The temperature and mass loss detection limit of the instrument was 1 °C and 0.001 mg, respectively. About 10 mg of powder sample was sealed in a standard aluminum pan in a dry nitrogen atmosphere. Non-isothermal DSC curves were recorded at the selected heating rate of 2, 4, 8, and 12 K min⁻¹ in the temperature range 323–673 K. Each sample was heated at four different heating rates and the change in heat flow as a function of temperature was recorded to determine the glass transition temperature (T_g), the peak crystallization temperature (T_p), onset crystallization temperature (T_c), and melting temperature (T_m).

Results and discussion

The glassy state of Se_{80.5}Bi_{1.5}Te_{18-y}Ag_y alloy is confirmed from the XRD pattern shown in Fig. 1. DSC scans for all investigated samples at a particular heating rate of 8 K min⁻¹ are reported in Fig. 2. Typical DSC curves of Se_{80.5}Bi_{1.5}Te_{16.5}Ag_{1.5} glass at four different heating rates are shown in Fig. 3. The DSC curves, shown in Figs. 2 and 3, are characterized by three regions representing glass transition region (endothermic phenomenon), crystallization process (exothermic phenomenon), and melting region (endothermic phenomenon). The appearance of single endothermic and exothermic peaks in the DSC curves indicates that the samples are homogeneous and exhibit a single phase [40]. The crystallization kinetics of any glassy material can be better understood in terms of its characteristic temperatures, i.e., glass transition T_g , onset crystallization T_c , peak crystallization T_p , and melting temperature T_m . Values of these temperatures with Ag concentration at different heating rates are reported in Table 1 which reveals that the characteristic temperatures T_g , T_c , and T_p increase with an increase in Ag content as well as with the heating rate. Similar results for other Ag-doped ternary chalcogenide glasses are reported [10, 41] in the literature. It has been found that T_g of a multi-component system depends upon several independent physical parameters, like coordination number, cohesive energy, bond energy, band gap, and effective molecular mass [10] of the material. The addition of Ag results in a heavily cross linked glass matrix, Se–Se bonds (bond energy

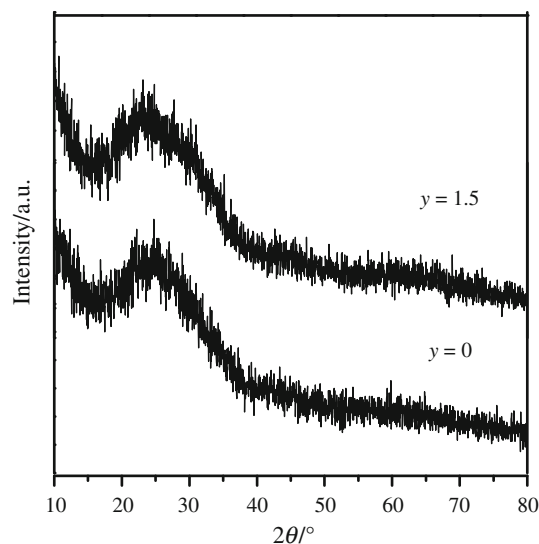


Fig. 1 X-ray diffraction pattern of Se_{80.5}Bi_{1.5}Te_{18-y}Ag_y glassy alloy for $y = 0$ and 1.5

183.92 kJ mol⁻¹) are replaced by Se–Ag bonds (bond energy 208.49 kJ mol⁻¹). It is in accordance with chemically ordered network model where the heteropolar bonds are favored over the homopolar bonds. Consequently, the addition of Ag escalates the cohesive energy of the system which leads to an increase in T_g of the system. Theoretically calculated values of transition temperature (T_g^{th}) are also given in Table 2 for comparison. The increase in T_g with Ag concentration may be ascribed to the increase in coordination number, cohesive energy, band gap, and molecular mass of the material. It is known that a very high cooling rate, during quenching, give rise to new configurational energy states. Various heating rates employed for DSC scans are different from the cooling rate used for quenching. The greater is the difference between these rates the larger is the structural differences. It has been reported [24] that higher heating rates offer higher T_g . From Table 1, it is observed that T_c increases with an increase in Ag concentration, its values are much higher than the room temperature. It means that Se_{80.5}Bi_{1.5}Te_{18-y}Ag_y glassy system prevent the self-transition of the material from one phase to another, i.e., crystalline to amorphous or vice versa, it is an essential feature for technological applications.

Glass transition activation energy

Glass transition temperature is a measure of strength and rigidity of a glassy network. Different methods are available in the literature to study the heating rate dependence of the T_g . The empirical relation proposed by Lasocka [42] relates the glass transition temperature to the heating rates β through the equation

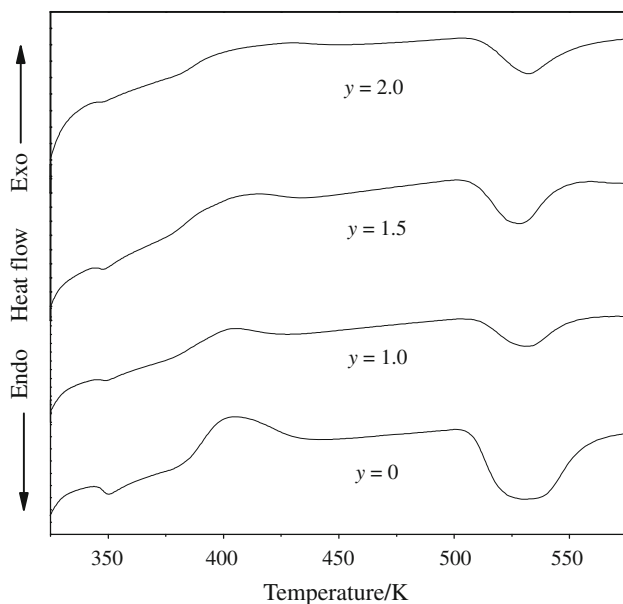


Fig. 2 DSC scans of $\text{Se}_{80.5}\text{Bi}_{1.5}\text{Te}_{18-y}\text{Ag}_y$ glasses at a heating rate of 8 K min^{-1}

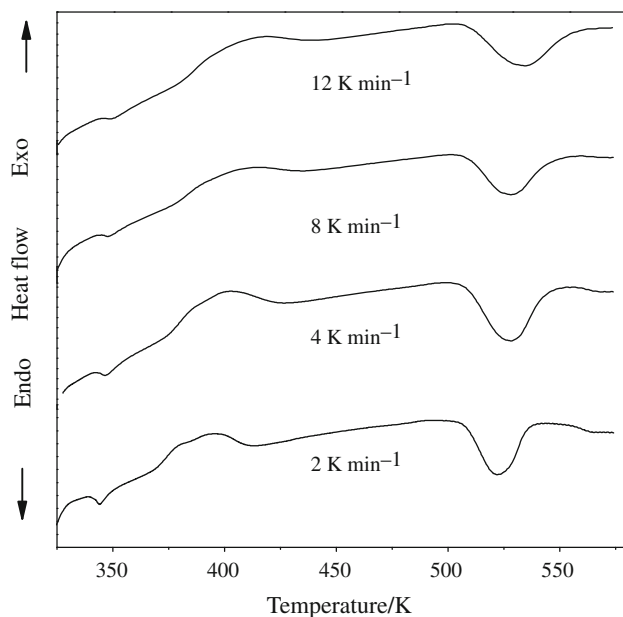


Fig. 3 DSC scans of $\text{Se}_{80.5}\text{Bi}_{1.5}\text{Te}_{16.5}\text{Ag}_{1.5}$ glass at different heating rates of 2, 4, 8, and 12 K min^{-1}

$$T_g = A + B \ln(\beta), \quad (1)$$

where A and B are the constants that depend on the material composition and heating rate used in DSC scans. The variation of T_g with $\ln(\beta)$ for all compositions is shown in Fig. 4. The constants A and B are evaluated from the intercept and slope of the plot. The calculated values of A and B are consistent with values reported for other chalcogenide glasses and are given in Table 2. Figure 4 reveals that the above equation is applicable and holds

good for all samples under study. Literature shows [42] that the constant B depends upon the cooling rate employed in the sample preparation and reflects the effect of heating rate on the structural changes within the glass transition region. The variation in the value of B, in Table 2, with Ag content demonstrates the configurational changes occurring in the samples with an increasing concentration of Ag. The second approach to study the heat dependence of T_g is the Kissinger formulation. In Kissinger formulation E_g can be obtained [34, 35] from the equation,

$$\ln\left(\frac{T_g^2}{\beta}\right) + \text{const.} = \frac{E_g}{RT_g}. \quad (2)$$

In Eq. (2), E_g is the glass transition activation energy and R is the universal gas constant. $\ln(T_g^2/\beta)$ as a function of $1,000/T_g$ for different compositions of $\text{Se}_{80.5}\text{Bi}_{1.5}\text{Te}_{18-y}\text{Ag}_y$ glass is found to be a straight line as shown in Fig. 5a. The slope of the plot gives the apparent activation energy E_g . Obtained values of E_g given in Table 2 illustrate that the energy of glass transition E_g increases with an increase in Ag contents. We have also studied the T_g and β dependence of E_g using Moynihan relation [36],

$$\ln(\beta) = -\frac{E_g}{RT_g} + \text{const.} \quad (3)$$

The activation energy E_g is obtained from the slope of the plot $\ln(\beta)$ versus $(1,000/T_g)$ shown in Fig. 5b. The calculated values of E_g for all four compositions are reported in Table 2 which make it clear that the values of E_g obtained by two methods are in agreement and increase with an increase in Ag content. These findings are in agreement with the earlier findings reported [10, 41] for Ag-doped chalcogenide glasses. Basically, E_g is the energy required by a group of atoms in glass transition region to jump from one metastable state to the other possible [43] metastable state. When the samples are heated in the furnace, during DSC scans, the atoms undergo infrequent transitions between local potential minimum separated by different energy barriers in the configurational space. Each local minimum represents a different structure and the most stable local minimum in the glassy region have lower internal energy. Accordingly, the atoms in the material with minimum activation energy have maximum probability to jump to a metastable state having minimum internal energy. $\text{Se}_{80.5}\text{Bi}_{1.5}\text{Te}_{18}$ glass has a minimum value of E_g , this particular glass has a larger probability to jump to a state of lower configurational energy state.

Crystallization activation energy and reaction order (n)

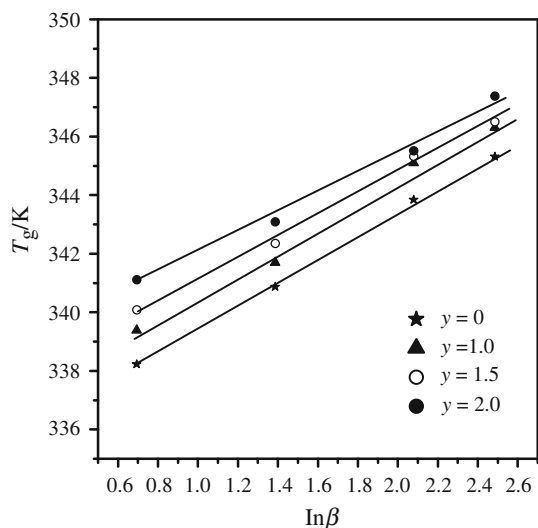
It is well known that the thermal stability and GFA of an amorphous alloy can be better understood in terms of the crystallization temperature T_c and activation energy of

Table 1 Values of characteristic temperatures, i.e., T_g , T_c and T_p , for $\text{Se}_{80.5}\text{Bi}_{1.5}\text{Te}_{18-y}\text{Ag}_y$, ($y = 0, 1.0, 1.5,$ and 2.0) glasses at heating rates of 2, 4, 8, and 12 K min^{-1}

Y	2 K min^{-1}			4 K min^{-1}			8 K min^{-1}			12 K min^{-1}		
	T_g/K	T_c/K	T_p/K	T_g/K	T_c/K	T_p/K	T_g/K	T_c/K	T_p/K	T_g/K	T_c/K	T_p/K
0	338.23	370.21	388.20	340.87	375.91	397.49	343.84	378.99	406.09	345.31	381.50	409.28
1.0	339.38	372.79	390.54	341.69	377.52	399.03	345.10	380.76	408.18	346.31	383.30	411.72
1.5	340.08	374.46	394.38	342.36	378.50	402.29	346.32	383.27	412.57	350.51	388.46	420.44
2.0	341.11	376.9	397.02	343.09	380.26	403.76	347.82	386.06	414.85	353.38	391.89	425.75

Table 2 Values of glass transition temperature T_g^{th} , activation energy of glass transition E_g , and kinetic parameters, A and B for $\text{Se}_{80.5}\text{Bi}_{1.5}\text{Te}_{18-y}\text{Ag}_y$ glasses

Composition	T_g^{th}/K	Glass activation energy $E_g/\text{kJ mol}^{-1}$		A/K	B/K
		Kissinger	Moynihan		
$\text{Se}_{80.5}\text{Bi}_{1.5}\text{Te}_{18}$	335.88	236.73 ± 14.8	242.42 ± 13.8	335.42 ± 1.1	4.0 ± 2.0
$\text{Se}_{80.5}\text{Bi}_{1.5}\text{Te}_{17}\text{Ag}_1$	340.85	237.22 ± 4.7	243.91 ± 5.7	336.47 ± 3.7	3.9 ± 0.6
$\text{Se}_{80.5}\text{Bi}_{1.5}\text{Te}_{16.5}\text{Ag}_{1.5}$	345.21	253.56 ± 11.4	264.89 ± 10.6	337.45 ± 2.4	3.6 ± 1.3
$\text{Se}_{80.5}\text{Bi}_{1.5}\text{Te}_{16}\text{Ag}_2$	348.32	269.75 ± 17.5	281.44 ± 16.7	338.51 ± 3.4	3.4 ± 1.8

**Fig. 4** Variation of T_g with heating rate $\ln(\beta)$ for amorphous $\text{Se}_{80.5}\text{Bi}_{1.5}\text{Te}_{18-y}\text{Ag}_y$ glasses

crystallization E_c . Hence, it is crucial to study the composition dependence of E_c and T_c . DSC is a valuable tool for the quantitative study of crystallization kinetics in amorphous materials. In literature, different methods have been employed by various researchers [34–39, 44] to estimate the activation energy of crystallization E_c . In amorphous materials, the crystallization mechanism can be controlled by nucleation and growth processes which are characterized by the activation energy of crystallization. First, we evaluate the activation energy of crystallization from the variation of the peak position of T_p by Kissinger's relation [34, 35], i.e.,

$$\ln\left(\frac{\beta}{T_p^2}\right) = -\frac{E_c}{RT_p} + \text{const.}, \quad (4)$$

where T_p is the peak crystallization temperature and E_c is the activation energy of crystallization. E_c has been determined from the slope of the plot $\ln(\beta/T_p^2)$ against $1,000/T_p$ shown in Fig. 6a. The graph between $\ln(\beta/T_p^2)$ and $(1,000/T_p)$ is a straight line, expected from the Eq. (4). The calculated values of E_c are given in Table 3. According to Mahadevan et al. [38], if the variation in $(1/T_p^2)$ with $\ln(\beta)$ is negligibly small compared to the variation in $(1/T_p)$, the above equation approximates [38] to

$$\ln(\beta) = -\frac{E_c}{RT_p} + \text{const.} \quad (5)$$

$\ln(\beta)$ as a function of $1,000/T_p$ for all compositions is plotted in Fig. 6b. The apparent activation energy E_c has been computed from the slope of these plots and the obtained values are given in Table 3. Augis and Bennett [37] have also proposed a method to determine the activation energy E_c by the relation

$$\ln\left(\frac{\beta}{T_p - T_0}\right) \cong \frac{-E_c}{RT_p} + \ln K_0, \quad (6)$$

where T_0 represents the onset temperature of crystallization and K_0 is frequency factor which measures the probability of molecular collision effective for the formation of the activated complex. In case, if $T_p \gg T_0$, the above equation reduced to the following relation [14],

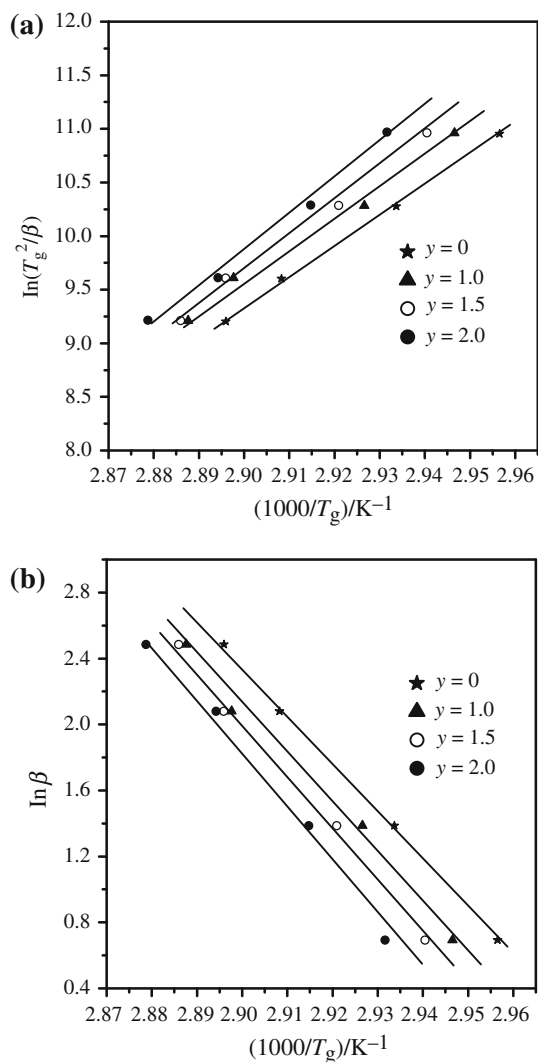


Fig. 5 Plot of **a** $\ln(T_g^2/\beta)$ versus $1,000/T_g$ and **b** $\ln(\beta)$ versus $1,000/T_g$ for $\text{Se}_{80.5}\text{Bi}_{1.5}\text{Te}_{18-y}\text{Ag}_y$ glasses

$$\ln\left(\frac{\beta}{T_p}\right) \cong \frac{-E_c}{RT_p} + \ln K_0. \quad (7)$$

$\ln(\beta/T_p)$ as a function of $1,000/T_p$ is plotted in Fig. 7. The plots of $\ln(\beta/T_p)$ versus $1,000/T_p$ are straight line and the slope of these plots gives E_c . The frequency factor K_0 may be computed from the intercept of the straight line with vertical axis. It is insisted that Augis and Bennett method is a conventional method for the determination of E_c because of its convenience and accuracy in the measurements of heating rates. In addition to E_c , this method also evaluates the frequency factor K_0 used for the description of phase transformation. The values of K_0 obtained for the samples under study along with E_c are reported in Table 3. The frequency factor K_0 is found to increase with increasing Ag content which makes it clear that the crystallization ability of $\text{Se}_{80.5}\text{Bi}_{1.5}\text{Te}_{18-y}\text{Ag}_y$ glass decreases with increasing

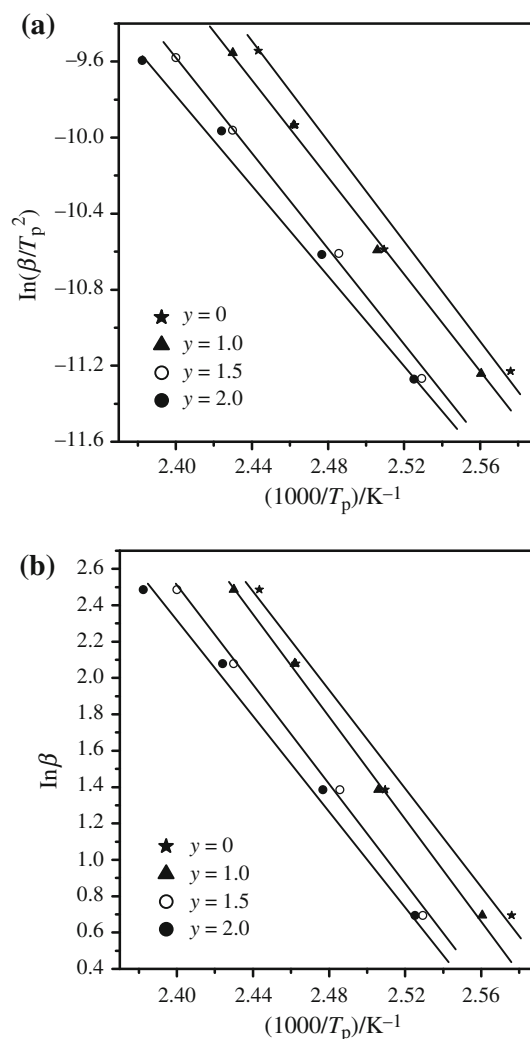


Fig. 6 Plot of **a** $\ln(\beta/T_p^2)$ versus $1,000/T_p$ and **b** $\ln(\beta)$ versus $1,000/T_p$ for $\text{Se}_{80.5}\text{Bi}_{1.5}\text{Te}_{18-y}\text{Ag}_y$ glasses

concentration of Ag. It is noticed that K_0 is maximum for $y = 2$ which implies that $\text{Se}_{80.5}\text{Bi}_{1.5}\text{Te}_{16}\text{Ag}_2$ glass has maximum resistance to crystallization.

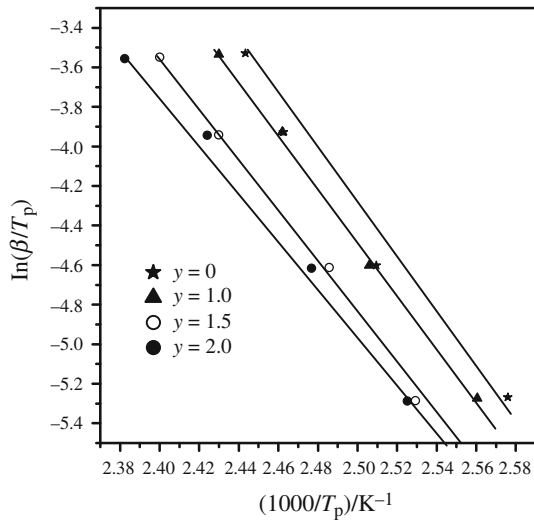
The most common model used to determine the activation energy of crystallization is JMA model [45–47], derived for isothermal conditions. Attempts are made to apply the JMA model for non-isothermal methods. In non-isothermal methods, Matusita et al. [39] has related the activation energy of crystallization to crystallized fraction heated at constant rate β by the relation [39]

$$\ln[-\ln(1 - \chi)] = -n \ln \beta - \frac{1.052mE_c}{RT} + \text{const.}, \quad (8)$$

where χ is the volume fraction of crystals precipitated in the chalcogenide glass heated at uniform rate. At a particular temperature, say T , the fraction χ is given as A_T/A , where A is the total area under the exotherm between the onset crystallization temperature T_i , where the

Table 3 Values of E_c , n , m , and K_0 in $\text{Se}_{80.5}\text{Bi}_{1.5}\text{Te}_{18-y}\text{Ag}_y$ glasses for different compositions

Composition	Crystallization activation energy $E_c/k \text{ J mol}^{-1}$				n	m	K_0/s^{-1}
	Kissinger	Mahadevan	Augis and Bennett	Matusita			
$\text{Se}_{80.5}\text{Bi}_{1.5}\text{Te}_{18}$	103.39 ± 10.2	110.02 ± 10.3	106.71 ± 10.2	114.08 ± 4.0	0.76903	1	2.21×10^{12}
$\text{Se}_{80.5}\text{Bi}_{1.5}\text{Te}_{17}\text{Ag}_1$	108.87 ± 3.5	115.53 ± 3.6	112.20 ± 3.7	116.46 ± 7.0	0.91975	1	2.65×10^{12}
$\text{Se}_{80.5}\text{Bi}_{1.5}\text{Te}_{16.5}\text{Ag}_{1.5}$	106.74 ± 4.4	113.49 ± 4.3	110.12 ± 4.4	110.72 ± 7.7	0.81478	1	5.24×10^{12}
$\text{Se}_{80.5}\text{Bi}_{1.5}\text{Te}_{16}\text{Ag}_2$	98.35 ± 5.6	105.13 ± 5.7	101.74 ± 5.5	105.90 ± 4.2	0.85814	1	1.40×10^{13}

**Fig. 7** Plot of $\ln(\beta/T_p)$ versus $1000/T_p$ for $\text{Se}_{80.5}\text{Bi}_{1.5}\text{Te}_{18-y}\text{Ag}_y$ glasses

crystallization just begin, and T_f where the crystallization is completed. A_T is the partial area under the exotherm between the temperature T_i and T . The particular temperature T is chosen in between T_i and T_f . m and n are constants that depend on the morphology of crystal growth mechanism and dimensionality of the glassy alloy. For the as-quenched alloys that contains no nuclei m is taken equal to $n - 1$. For the glass containing sufficiently large number of nuclei m is taken equal to n . In our case $m = n - 1$ because we are investigating the as-quenched samples that contains no nuclei. A plot of $\ln[-\ln(1 - \chi)]$ versus $\ln(\beta)$, at fixed temperature, yields a straight line as shown in Fig. 8a. The slope of this line gives the Avrami exponent n . The average value of n obtained from the slopes of the plots shown in Fig. 8a is given in Table 3. For the as-quenched sample n can have values between 1 and 4, depending upon the crystallization mechanism occurring in the material. $n = 1, 2, 3$, and 4, respectively represent surface nucleation with one dimensional growth from surface to inside, volume nucleation with one dimensional growth, volume nucleation with two dimensional growth, and volume nucleation with three dimensional growth. Once, the molten material is cooled, the relaxation time for molecular movements becomes comparable to the experimental timescale. Consequently, the

diffusive motion of the liquid is trapped and the material falls out of the thermal equilibrium [48]. At this stage, the size of the nuclei does not attain the size required to initiate the nucleation process and the glass formed is assumed to have no nuclei. Matusita has shown that when the glass is heated in a DSC furnace, the rate of nucleation reaches maximum at a temperature higher than the glass transition temperature and decreases rapidly with further increase in temperature. During constant heating rate, the formation of crystal nuclei occur at a lower temperature and the crystals grow in size at a higher temperature without increasing in number. Also, the presence of sharp peak (T_p) during crystallization process, which shifts toward higher temperatures with increasing heating rates, indicates that the system does not get sufficient time for nucleation and crystallization. The process of nucleation and crystal growth in these materials, during amorphous to crystalline phase transformation, can be explained in terms of the Avrami parameter n . For samples under study, n has been found to lie between 0.78 and 0.92, i.e., $n \sim 1$. This means that during amorphous-crystallization phase transformation $\text{Se}_{80.5}\text{Bi}_{1.5}\text{Te}_{18-y}\text{Ag}_y$ chalcogenide glass involve surface nucleation with one dimensional growth from surface to inside.

Figure 8b shows the plot of $\ln[-\ln(1 - \chi)]$ as a function of $1000/T$ at different heating rates for $y = 1.5$. The deviation from the straight line is may be due to the saturation of nucleation sites during crystallization. The slope of the plot $\ln[-\ln(1 - \chi)]$ versus $1000/T$ gives the value of mE_c . Since no heat treatment is given to the samples before the DSC measurements, m can be taken as 1. The activation energy of crystallization for $\text{Se}_{80.5}\text{Bi}_{1.5}\text{Te}_{18-y}\text{Ag}_y$ glasses, calculated from the average value of m and mE_c , is reported in Table 3. It is observed that the values of E_c obtained from the Matusita method are higher than the values obtained by other methods. In this method, E_c is obtained from the variation in temperature that scans the entire curve from beginning of the crystallization process till its end. It also allows in determining the crystallization mechanism involved and dimensionality of growth.

From Table 3, one can see that the value of activation energy of crystallization decreases with an increase in Ag concentration. The variation in the value of activation energy of crystallization describes the structural changes

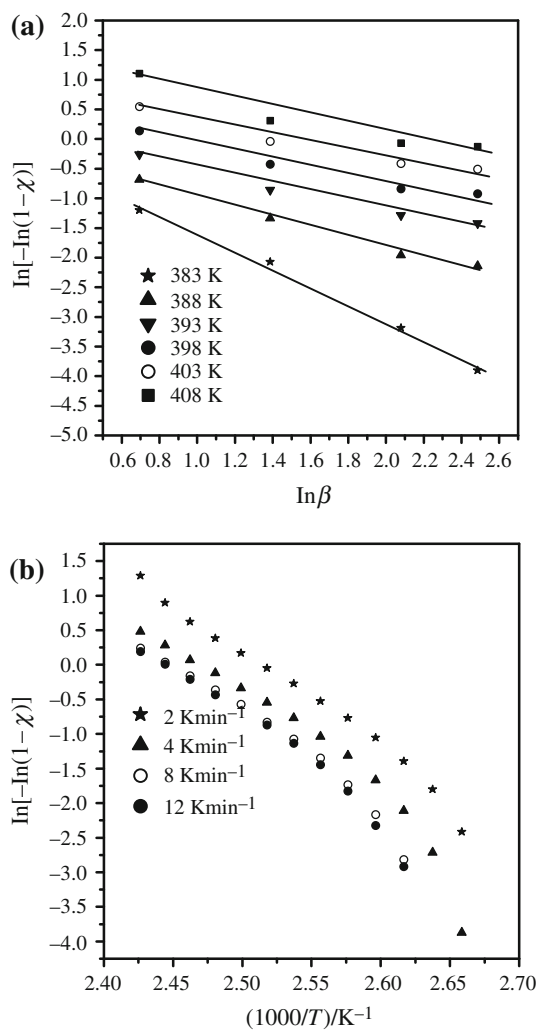


Fig. 8 Plot of **a** $\ln[-\ln(1-\chi)]$ versus $\ln(\beta)$ at fixed temperature and **b** $\ln[-\ln(1-\chi)]$ versus $1000/T$ for $\text{Se}_{80.5}\text{Bi}_{1.5}\text{Te}_{16.5}\text{Ag}_{1.5}$ glass

occurring in the samples under study. The activation energy of crystallization is also an indication of the speed of crystallization. From Table 3, it is evident that E_c , calculated from all methods, follows the similar trend. The difference in the values of E_c in different formalisms may be attributed to the different approximations used in these formalisms. Further, an increase in Ag concentration leads

to the decrease in E_c as evident from Table 3. For $y = 2$, the value of E_c is minimum in all formalisms. This decrease in E_c may be due to the fact that the addition of more Ag results in heavy cross-linked structure due to the cross linking of Ag with other elements. It reduces the tendency of crystallization and a decrease in E_c is observed. The small value of E_c for $y = 2$ indicates a decrease in the speed of crystallization and an increase in resistance to crystallization as evident from the frequency factor K_0 .

Thermal stability and glass forming ability

From technology point of view, the chalcogenide material should be thermally stable and good glass former. Glass-forming ability is an important parameter to determine the degree of utilization of the material in various technological applications. For memory and switching applications, thermal stability and GFA are of vital importance. Different quantitative methods are used [49–51] by the researcher to study the stability of a glass using characteristic temperatures such as transition temperature T_g , crystallizations temperature T_c , peak crystallization temperature T_p , and the melting temperature T_m . Dietzel [52] has introduced an important parameter, $\Delta T = T_c - T_g$, to know the GFA of the glassy materials. The values of ΔT for different compositions are given in Table 4 which reveals that ΔT increases with an increasing content of Ag. It is found that ΔT has maximum for $\text{Se}_{80.5}\text{Bi}_{1.5}\text{Te}_{16}\text{Ag}_2$ glass which shows that the glass with 2 % of Ag is thermally more stable. In the case of non-isothermal study, the thermal stability of the glass may also be understood in terms of the difference between T_p and T_g . Large difference in T_p and T_g indicates delay in the nucleation process [53]. So, the difference $(T_p - T_g)$ is a measure of thermal stability and GFA of the material against crystallization. Higher values of $(T_p - T_g)$ imply greater thermal stability and GFA because higher value of $(T_p - T_g)$ means large resistance to crystallization. It is found that this difference has maximum for $y = 2$, it means that $\text{Se}_{80.5}\text{Bi}_{1.5}\text{Te}_{16}\text{Ag}_2$ glass is more stable and has maximum GFA, supported by ΔT , compared to other compositions. This shows that

Table 4 Values of $(T_c - T_g)$, $(T_p - T_g)$, and stability parameters H_R , H_w , and S at 8 and 12 K min^{-1} for different compositions of $\text{Se}_{80.5}\text{Bi}_{1.5}\text{Te}_{18-y}\text{Ag}_y$ glasses

Y	8 K min^{-1}					12 K min^{-1}				
	$T_c - T_g/\text{K}$	$T_p - T_g/\text{K}$	H_R	H_w	S	$T_c - T_g/\text{K}$	$T_p - T_g/\text{K}$	H_R	H_w	S
0	35.15	62.25	0.279	0.102	2.77	36.19	63.97	0.290	0.105	2.912
1	35.66	63.08	0.285	0.103	2.83	37.00	65.41	0.301	0.107	3.036
1.5	36.95	66.25	0.296	0.107	3.13	37.95	69.93	0.316	0.108	3.463
2.0	38.24	67.03	0.310	0.110	3.17	38.51	72.37	0.322	0.109	3.689

Se_{80.5}Bi_{1.5}Te₁₆Ag₂ glass has lesser tendency to crystallization, revealed by decrease in the value of E_c , and increase in the value of K_0 . Using the characteristic temperatures Hruby [50] developed a parameter

$$H_R = \frac{\Delta T}{T_m - T_c}, \quad (9)$$

as an indicator of GFA. On the other hand, Saad and Poulain [51] introduced two parameters that can also be used to study the thermal stability of a glass. These parameters are

$$H_w = \frac{\Delta T}{T_g}, \quad (10)$$

called weighted thermal stability and

$$S = \frac{(T_p - T_c)(T_c - T_g)}{T_g}. \quad (11)$$

The thermal stability of the samples under study is also estimated from these two parameters. The values of stability and GFA parameters H_R , H_w , and S are reported in Table 4. It is found that the values of these parameters increase with an increase in Ag concentration as well as with the heating rate. The thermal stability of a glass can also be understood in terms of variation of T_c and $(T_c - T_g)$. Values of T_c and $(T_c - T_g)$ for different compositions are given in Tables 1 and 4, respectively. From Table 4, it is observed that $(T_c - T_g)$ increases with an increase in Ag concentration and is maximum for $y = 2$. It shows that the thermal stability of glass increases with increasing concentration of Ag in the glass. From the above discussion, it is deduced that the addition of Ag in Se–Te–Bi glass improves its thermal stability as well as the GFA. Similar findings for other Ag-doped chalcogenide glasses are reported in literature [10, 41]. The increase in the thermal stability of Se_{80.5}Bi_{1.5}Te_{18-y}Ag_y chalcogenide glasses may be attributed to the increase in the cohesive energy of the material [54] with an increase in Ag concentration. Kauzmann [55] has given another criterion to estimate the GFA in terms of reduced transition temperature, i.e., $T_{rg} \geq 2/3$, called two-third rule. The ease of glass formation is determined by calculating T_{rg} from the relation

$$T_{rg} = \frac{T_g}{T_m}, \quad (12)$$

where T_m is the melting temperature. For the samples under study, the value of reduced temperature is found to be $\geq 2/3$ (not given here), which shows that the two-third rule holds well for all compositions under study. It means that Se_{80.5}Bi_{1.5}Te_{18-y}Ag_y glass has good GFA for all the compositions under study.

Conclusions

Crystallization kinetics of Se_{80.5}Bi_{1.5}Te_{18-y}Ag_y chalcogenide glass for $y = 0, 1.0, 1.5$, and 2.0 at.% has been studied at four different heating rates using differential scanning calorimetric measurement. The characteristic temperatures, i.e., glass transition temperature, T_g , onset crystallization temperature, T_c , and peak crystallization temperature, T_p , are found to increase with an increase in Ag concentration as well as with the heating rate. The activation energy of glass transition E_g determined from two approaches is in agreement with each other and is found to increase with increasing Ag content. The activation energy of crystallization E_c evaluated by four different methods is in agreement and follows the similar trend. An increase in the concentration of Ag results in the formation of heavy cross linked structure in the material which lead to the retarded tendency of crystallization, evidenced by $(T_p - T_g)$, K_0 , and E_c . The average value of Avrami index shows that amorphous-crystalline transformation in the samples under investigation is associated with surface nucleation with one dimensional growth from surface to inside. Characteristic temperatures are used to determine the thermal stability and the ease of glass formation. The maximum value of $(T_p - T_g)$ and $(T_c - T_g)$ for Se_{80.5}Bi_{1.5}Te₁₆Ag₂ glass shows that it is more stable compared to the other compositions under study. The thermal stability and GFA parameters, i.e., H_R , H_w , and S also show that Se_{80.5}Bi_{1.5}Te₁₆Ag₂ glass is more stable than the other glasses under investigation. Thus, from the above discussion, we can conclude that the addition of Ag to Se–Te–Bi system makes the system thermally more stable. The increase in the thermal stability and GFA of Se_{80.5}Bi_{1.5}Te_{18-y}Ag_y glasses with addition of Ag may be ascribed to the increase in cohesive energy with increasing silver concentration.

Acknowledgments We are thankful to Prof. Kulvir Singh, Thaper University Patiala, for scanning our samples on Diamond Pyris (Perkin Elmer) DSC and valuable suggestions regarding the work.

References

1. Wang MF, Jang MS, Huang JC, Lee CS. Synthesis and characterization of quaternary chalcogenides InSn₂Bi₃Se₈ and In_{0.2}Sn₆Bi_{1.8}Se₉. *J Solid State Chem.* 2009;182:1450–6.
2. Yahia IS, Hegab NA, Shakra AM, Al-Ribaty AM. Conduction mechanism and the dielectric relaxation process of a-Se₇₅Te_{25-x}Ga_x ($x = 0, 5, 10$ and 15 at wt%) chalcogenide glasses. *Phys B Phys Condens Matter.* 2012;407:2476–85.
3. Singh AK. A short over view on advantage of chalcogenide glassy alloys. *J Non Oxide Glasses.* 2012;3:1–4.
4. Chandel N, Mehta N, Kumar A. Investigation of a. c. conductivity measurements in a-Se₈₀Te₂₀ and a-Se₈₀Te₁₀M₁₀ (M = Cd, In, Sb) alloys using correlated barrier hopping model. *Curr Appl Phys.* 2012;12:405–12.

5. Ahmad M, Thangaraj R, Sathiaraj TS. Heterogeneous crystallization and composition dependence of optical parameters in Sn–Sb–Bi–Se chalcogenides. *J Mater Sci.* 2010;45:1231–6.
6. Kotkata MF, Mansour A. Study of glass transition kinetics of selenium matrix alloyed with up to 10 % indium. *J Therm Anal Calorim.* 2011;103:555–61.
7. Wakkad MM. Crystallization kinetics of $Pb_{20}Ge_{17}Se_{63}$ and $Pb_{20}Ge_{22}Se_{58}$ chalcogenide glasses. *J Therm Anal Calorim.* 2001;63:533–47.
8. Gao YQ, Wang W. On the activation energy of crystallization in metallic glasses. *J Non Cryst Solids.* 1986;81:129–34.
9. Deepika, Jain PK, Rathore KS, Saxena N. Structural characterization and phase transformation kinetics of $Se_{58}Ge_{42-x}Pb_x$ ($x = 9, 12$) chalcogenide glasses. *J Non Cryst Solids.* 2009;355:1274–80.
10. Al-Ghamdi AA, Alvi MA, Khan SA. Non-isothermal crystallization kinetic study on $Ga_{15}Se_{85-x}Ag_x$ chalcogenide glasses by using differential scanning calorimetry. *J Alloys Compd.* 2011;509:2087–93.
11. Marseglia EA, Davis EA. Crystallization of amorphous selenium and $As_{0.005}Se_{0.995}$. *J Non Cryst Solids.* 1982;50:13–21.
12. Matsur M, Suski K. Kinematical transformations of amorphous selenium by DTA measurement. *J Mater Sci.* 1979;14:395–400.
13. Surinach S, Baro MD, Clavaguera-Mora MT, Clavaguera N. Kinetic study of isothermal and continuous heating crystallization in $GeSe_2GeTeSb_2Te_3$ alloy glasses. *J Non Cryst Solids.* 1983;58:209–17.
14. Yinnon H, Uhlmann DR. Applications of thermoanalytical techniques to the study of crystallization kinetics in glass-forming liquids, part I: theory. *J Non-Cryst Solids.* 1983;54:253–75.
15. Chander R, Thangaraj R. Thermal and optical analysis of Te-substituted Sn–Sb–Se chalcogenide semiconductors. *J Appl Phys A.* 2010;99:181–7.
16. Joraid AA. The effect of temperature on non-isothermal crystallization kinetics and surface structure of selenium thin films. *Phys B.* 2007;390:263–9.
17. Lopez-Almany PL, Vazquez J, Villares P, Jimnez-Garay R. Application of the single-scan calorimetric technique to the crystallization of the semiconducting $Sb_{(0.16)}As_{(0.29)}Se_{(0.55)}$ alloy. *J Non Cryst Solids.* 2001;287:171–6.
18. Joraid AA, Alamri SN, Abu-Sehly AA. Model-free method for analysis of non-isothermal kinetics of a bulk sample of selenium. *J Non Cryst Solids.* 2008;354:3380–7.
19. Kumar S, Singh K. Glass transition, thermal stability and glass forming tendency of $Se_{90-x}Te_5Sn_5In_x$ multi-component chalcogenide glasses. *Thermochim Acta.* 2012;528:32–7.
20. Dohare C, Mehta N, Kumar A. Effect of some metallic additives (Ag, Cd, Zn) on the crystallization kinetics of glassy $Se_{70}Te_{30}$ alloy. *Mater Chem Phys.* 2011;127:208–13.
21. Li B, Xie Y, Xu Y, Wu C, Li Z. Selected-control solution-phase route to multiple-dendritic and cuboidal structures of PbSe. *Solid State Chem.* 2006;179:56–61.
22. Sharma A, Barman PB. Effect of Bi incorporation on the glass transition kinetics of $Se_{85}Te_{15}$ glassy alloy. *J Therm Anal Calorim.* 2009;96:413–7.
23. Hrdlicka M, Prikryl J, Pavlista M, Benes L, Vlcek M, Frumar F. Optical parameters of In–Se and In–Se–Te thin amorphous films prepared by pulsed laser deposition. *J Phys Chem Solids.* 2007;68:846–9.
24. Abdel-Wahab Fouad. Observation of phase separation in some Se–Te–Sn chalcogenide glasses. *Phys B.* 2011;406:1053–9.
25. Nagels P, Tichy L, Tiska A, Ticha H. Photoconductivity of vitreous chalcogenides chemically modified by bismuth. *J Non Cryst Solids.* 1983;50–60:999–1002.
26. Toghe N, Yamamoto Y, Minami T, Tanka M. Preparation of n type semiconducting $Ge_{20}Bi_{10}Se_{70}$ glass. *J Appl Phys Lett.* 1979;34:640–1.
27. Mitkova M, Boncheva-Mladenova Z. Glass-forming region and some properties of the glasses from the system Se–Te–Ag. *Monatshfte fuer Chemie.* 1989;120:643–50.
28. Frumar M, Wagner T. Ag doped chalcogenide glasses and their applications. *Curr Opin Solid State Mater Sci.* 2003;7:117–26.
29. Garrido JMC, Macoretta F, Urena MA, Arcondo Z. Application of Ag–Ge–Se based chalcogenide glasses on ion-selective electrodes. *J Non Cryst Solids.* 2009;355:2079–82.
30. Piarristeguy AA, Cuello GJ, Arcondo B, Pradel A, Ribes M. Neutron thermodiffraction study of silver chalcogenide glasses. *J Non Cryst Solids.* 2007;353:1243–6.
31. Shakra AM, Fayek SA, Hegab NA, Yahia IS, AL-Ribaty AM. Crystallization kinetics of a- $Se_{75}Te_{25-x}Ga_x$ ($x = 0, 5, 10$ and 15 at wt%) glassy system. *J Non Cryst Solids.* 2012;358:1591–8.
32. Dohare C, Mehta N. Investigation of crystallization kinetics in glassy Se and binary $Se_{98}M_2$ ($M = Ag, Cd, Zn$) alloys using DSC technique in non-isothermal mode. *J Cryst Proc Technol.* 2012;2:167–74.
33. Schubert J, et al. Multi component thin films for electrochemical sensor applications prepared by pulsed laser deposition. *Sens Actuators B Chem B.* 2001;76:327–30.
34. Kissinger HE. Variation of peak temperature with heating rate in differential thermal analysis. *J Res Natl Bur Stand.* 1956;57:217–21.
35. Kissinger HE. Reaction kinetics in differential thermal analysis. *Anal Chem.* 1957;29:1702–6.
36. Mohynihan CT, Easteal AJ, Wilder J, Tucker J. Dependence of the glass transition temperature on heating and cooling rate. *J Phys Chem.* 1974;78:2673–7.
37. Augis JA, Bennett JE. Calculation of the Avrami parameters for heterogeneous solid state reactions using a modification of the Kissinger method. *J Therm Anal Calorim.* 1978;13:283–92.
38. Mahadevan S, Giridhar A, Singh AK. Calorimetric measurements on As–Sb–Se glasses. *J Non Cryst Solids.* 1986;88:11–34.
39. Matusita K, Konatsu T, Yokota R. Kinetics of non-isothermal crystallization process and activation energy for crystal growth in amorphous materials. *J Mater Sci.* 1984;19:291–6.
40. Patial BS, Thakur N, Tripathi SK. On the crystallization kinetics of In additive Se–Te chalcogenide glasses. *J Thermochim Acta.* 2011;513:1–8.
41. Bindra KS, Suri N, Kamboj MS, Thangaraj P. Calorimetric analysis of Ag doped amorphous Se–Sb chalcogenide glasses. *J Ovonic Research.* 2007;3:1–13.
42. Lasocka M. The effect of scanning rate on glass transition temperature of splat-cooled $Te_{85}Ge_{15}$. *Mater Sci Eng.* 1976;23:173–7.
43. Imran MMA, Bhandari D, Saxena NS. Enthalpy recovery during structural relaxation of $Se_{96}In_4$ chalcogenide glass. *Phys B.* 2001;293:394–401.
44. Patial BS, Thakur N, Tripathi SK. Crystallization study of Sn additive Se–Te chalcogenide alloys. *J Therm Anal Calorim.* 2011;106:845–52.
45. Avrami M. Kinetics of phase change.-I general theory. *J Chem Phys.* 1939;7:1103–12.
46. Avrami M. Kinetics of phase change. II. Transformation-time relations for random distribution of nuclei. *J Chem Phys.* 1940;8:212–24.
47. Avrami M. Granulation, phase change and microstructure kinetics of phase change III. *J Chem Phys.* 1941;9:177–84.
48. Imran MMA, Saxena NS, Husain M. Glass transition phenomena, crystallization kinetics and enthalpy released in binary $Se_{100-x}In_x$ ($x = 2, 4$ and 10) semiconducting glasses. *Phys Status Solid A.* 2000;181:357–68.
49. Uhlmann DR. A kinetic treatment of glass formation. *J Non Cryst Solids.* 1972;7:337–48.
50. Hruby A. Evaluation of glass-forming tendency by means of DTA. *Czechoslov J Phys B.* 1972;22:1187–93.

51. Saad M, Poulain M. Glass forming ability criterion. *Mater Sci Forum*. 1987;19–20:11–8.
52. Dietzel A. Glass structure and glass properties. *Glasstech Ber*. 1968;22:41–50.
53. Mehta N, Tiwari RS, Kumar A. Glass forming ability and thermal stability of some Se–Sb glassy alloys. *Mater Res Bull*. 2006;41:1664–72.
54. Kumar A, Heera P, Sharma P, Barman PB, Sharma R. Compositional dependence of optical parameters in Se–Bi–Te–Ag thin films. *J Non Cryst Solids*. 2012;358:3223–8.
55. Kauzmann W. The nature of the glassy state and the behavior of liquids at low temperatures. *Chem Rev*. 1948;43:219–56.